A new modal-based damage location indicator

G.R. Gillich[1], Z.I. Praisach[1], M. Abdel Wahab[2], H. Furdui[1]
[1] Eftimie Murgu University of Resita, Department of Mechanical Engineering
P-ta Traian Vuia 1-4, 320085, Resita, Romania
e-mail: **gr.gillich@uem.ro**

[2] Department of Mechanical Construction and Production, Faculty of Engineering and Architecture, Ghent University, Technologiepark Zwijnaarde 903, B-9052 Zwijnaarde, Belgium

Abstract
Vibration-based damage detection techniques use the change in modal data as an indicator to assess damages in the structure. Knowing the structural dynamic characteristics of the healthy and damaged structure, the estimation of the damage location and severity is possible by solving an inverse problem. This paper presents a mathematical expression relating damage location and depth to the frequency shifts of the bending vibration modes. This expression permits the extraction of a series of coefficients that characterize each damage location and are independent of the damage severity. The vector aggregating these coefficients for a given location constitutes a Damage Location Indicator (DLI) that unambiguously characterizes the position of a geometrical discontinuity in the beam. A set of vectors typifying all locations along the beam may be used as patters opposable to the damage signature found by measurements. The similarity between the signature and one of the patterns indicates the location of damage.

1 Introduction

Monitoring of structures to assess their integrity has been one of the most important issues in civil and mechanical engineering in the last years. Numerous non-destructive techniques are now available, permitting to achieve one of the following damage assessment levels: a) detection, b) localization and c) severity. The vibration-based methods associate damage with changes in the dynamic response of structures, which occur due to the decreased beam capacity to store energy. The link between a damage and the changes in the structural response is described by mathematical expressions reflecting various models, from analytical beam models to statistical models predicting the beam dynamic behavior. Often the response changes refer to the natural frequencies, but other modal parameters can also be involved in damage detection algorithms.

Extensive literature reviews on this topic are presented by Doebling et al. [1] and Sohn et al. [2]. They focused on methods and data required for damage identification by examining the changes in various types of measured structure responses. The use of inverse methods in damage detection using measured vibration data is presented by Friswell [3], who made a critical review on problems occurring with this approach, including modeling errors and environmental effects.

Methods destined to predict the damage location and evaluate its severity are usually model-based. Various damage modeling approaches are presented in literature; see for instance Fritzen [4], Friswell [5], Dimarogonas [6] and Ostachowicz and Krawczuk [7] and Christides and Barr [8]. All these approaches can be classified into three main categories; nalely local stiffness reduction, discrete spring models, and complex models in two or three dimensions. The discontinuity is often considered as an open crack, in order to neglect the nonlinear effects due to a crack closure. Other authors like Yan et al. [9] considered a bilinear behavior of closing cracks. However, no models precisely predicting frequency changes due to discontinuities for a large number of vibration modes are available. Furthermore, the use of existing

models requires time for fitting the models to particular applications, in order to utilize them for damage detection. Additionally, for higher vibration modes important computational resources are needed to numerically solve the characteristic equations, which can impose a serious constrain.

This paper presents the results of a study aiming to formulate the relation between damage location and depth, and the frequency shifts. While the frequency in any mode depends on its stored energy, the idea is to compare the frequency decrease for the bending modes with the loss of its energy. The frequencies of a slender double clamped beam in healthy and damaged states are found, for numerous locations along the beam, by means of the finite element analysis and frequency shift curves plotted for the first eight weak-axis bending vibration modes. These curves are compared with curves representing the energy distribution of the healthy beam, analytically determined, and a perfect agreement is found. This permits to write a mathematical expression that predicts the frequency change due to a certain damage by considering the healthy state of the beam alone, in terms of modal energy distribution. Furthermore, it is possible to decouple the effect of the damage location from that of the damage severity. Thus, from the frequency changes in the first several bending vibration modes, parameters characterizing a damage location and a pattern describing the behavior due to the damage at that location are obtained. Comparing patterns obtained in this way with measured frequency shifts, it is possible to identify precisely that location of damage.

2 The Damage Location Indicators

Since natural frequencies are the most facile acquirable data characterizing the beam dynamics behavior, we focused our research on this feature. The basic idea in damage assessment using the natural frequencies of a structure reckons on the fact that any change in the structure causes a change in its frequencies. The relationship between physical parameters and the natural frequencies f_i of a healthy beam is:

$$f_i = \frac{\lambda_i^2}{2\pi}\sqrt{\frac{EI}{\rho A L^4}} \tag{1}$$

where λ_i is the wave number of the i-th bending vibration mode, E is the Young's modulus, I is the moment of inertia of the weak-axis, A is the cross-sectional area, ρ is the mass density and L the beam length. Any structural change will affect one or more physical parameters, and consequently upon the natural frequencies. Some theoretical models, for instance in references [10] and [11], considered a "continuous" approach, where the beam is spited into two segments linked by a torsional massless spring. To derive the frequency shift due to damage with a given depth and location, it is necessary to replace the damage and adjust its stiffness for each case separately. To have an overview about what happens in numerous damage scenarios, it implies solving a large number of differential equations that usually require a great effort. Our researches were focused in finding an easier way to derive the frequency changes. Considering that a certain damage produce the same local effect in any location along the structure, and the result on the global dynamic behavior of the structure depends on damage location, we searched for a relation that consider the damage severity as a constant for a given depth, adjusted by a function to provide the effect of damage location.

2.1 Numerical analysis of a clamped-clamped beam

To find the frequency changes for a large number of bending vibration modes, in case of damages with different depths and located consecutively on numerous locations along the beam, a finite element analysis using the ANSYS program is performed. This paper present the case of a double clamped steel beam, having a length L = 1 m, width B = 0.05 m and height H = 0.005 m, cross-section $A = 250\cdot10^{-6}$ m^2 and the moment of inertia $I = 520.833\cdot10^{-12}$ m^4 for the undamaged state. The material parameters are: mass density ρ = 7850 kg/m^3; Young's modulus $E = 2.0\cdot10^{11}$ N/m^2 and Poisson's ratio μ = 0.3.

For the damage scenarios we considered around 198 damage locations equidistantly placed along the beam, while the breathing cracks had successively 9 levels of depth. Consequently we obtained for eight vibration modes the frequency shifts for 1782 damage scenarios. Figure 1 present, for the double clamped beam, the frequency shift curves for four levels of depth, namely healthy beam and cross-section reduction with 42%, 50% and 58% respectively.

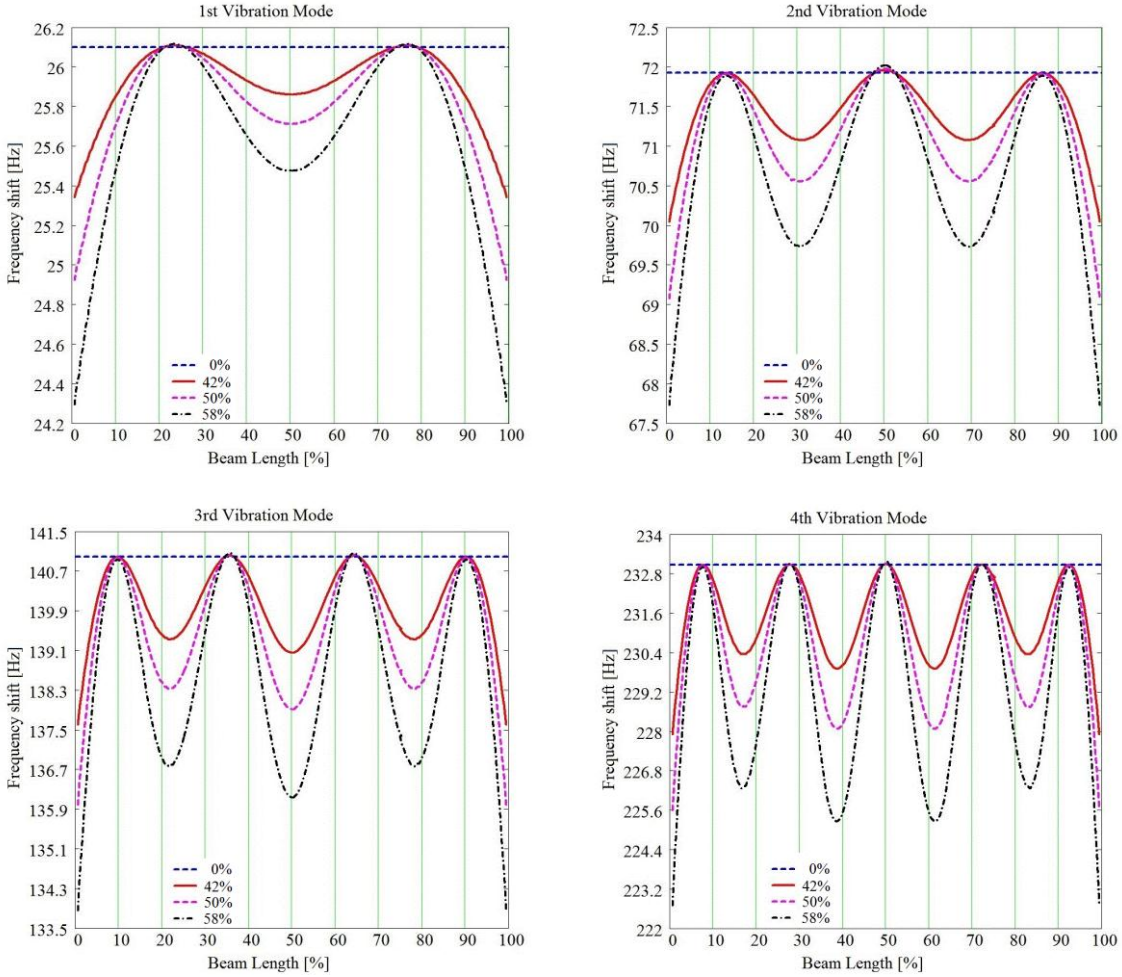

Figure 1: Frequency shift curves for modes 1 to 4 for three depth damage levels.

From Figure 1, one observes that there are, for a given vibration mode, locations where a damage produces no frequency changes, irrespective to damage depth, while for other locations the frequency changes exhibit local maxima. These points are different for each vibration mode, but similar as relative position *x/L* for a given mode for beams having the same support type. For instance a double clamped beam with a damage placed at $x/L = 0.2765$ undergo no change in frequency for the fourth vibration mode, whereas at $x/L = 0.6333$, the frequency change exhibits a local maxima.

It can be presumed that the phenomenon can be explained by considering the way how the beam slices contribute to the total potential stored energy in each vibration mode. The slices placed in the vicinity of inflection points of the mode shape curvature, where the bending moment is null, do not contribute to the total potential stored energy. Opposite, slices placed on local maxima of the mode shape curvature, in other words the local maxima of the bending moment, suffer important deflections and accumulate therefore the highest values of potential stored energy, substantially contributing to the total value of this energy. These presumptions are supported by Eq. (2) describing the strain energy and Figure 2, where the similitude between the beam characteristic points and frequency shifts is depicted.

$$dU_i(x) = \frac{1}{2} EI\left(\phi_i''(x)\right)^2 dx \tag{2}$$

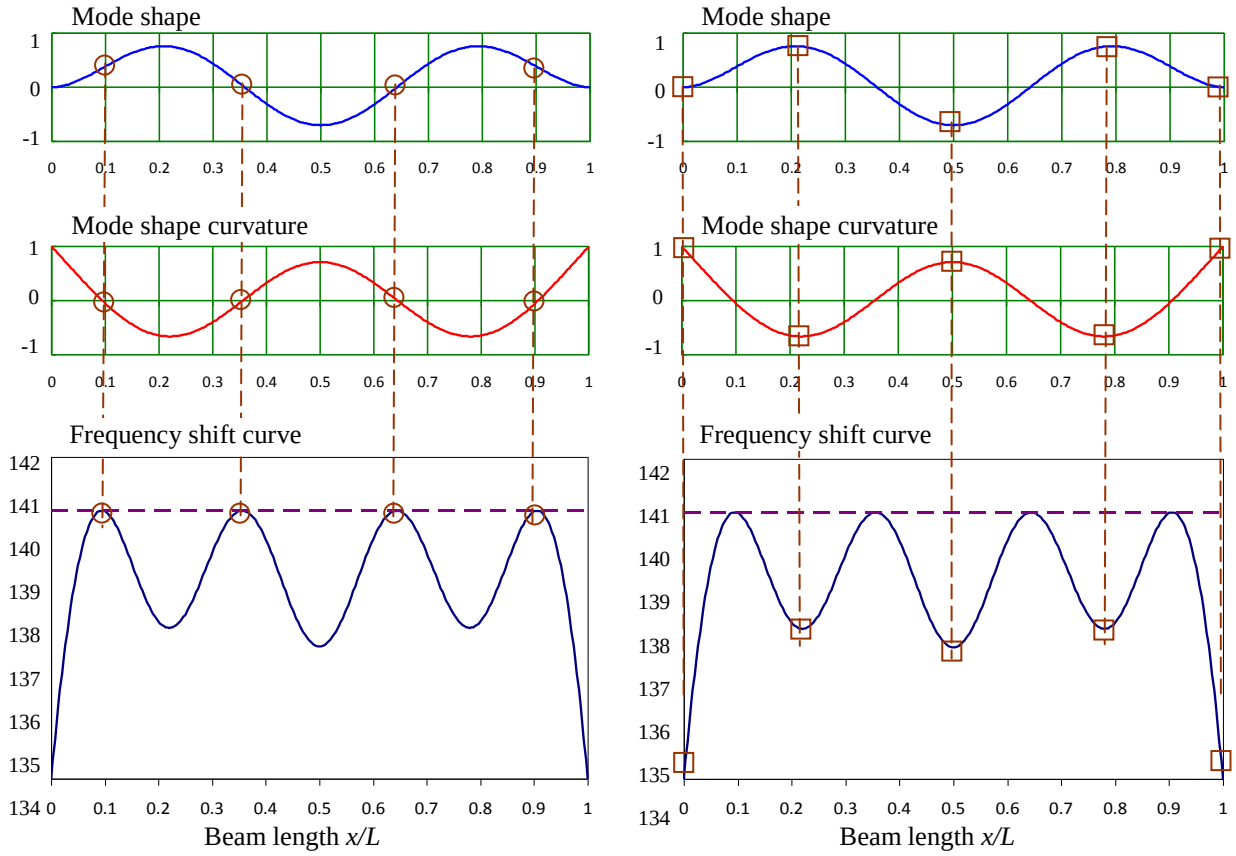

a) b)

Figure 2: The behavior of beam slices relative to their location on the beam for vibration mode 3

In Figure 2, the curves representing the mode shapes $\phi_i(x)$ and their second derivatives $\phi_i''(x)$, i.e. the mode shape curvatures, are plotted using the well-known relations presented in Eqs. (3) and (4), that are

$$\phi_i(x) = (\cos\alpha_i x - \cosh\alpha_i x) + \xi \cdot (\sin\alpha_i x - \sinh\alpha_i x) \tag{3}$$

$$\phi_i''(x) = (\cos\alpha_i x + \cosh\alpha_i x) + \xi \cdot (\sin\alpha_i x + \sinh\alpha_i x) \tag{4}$$

where we denoted $\frac{\rho A\omega^2}{EI} = \frac{\lambda^4}{L^4} = \alpha^4$ and $\xi = \frac{\sin\alpha_i L + \sinh\alpha_i L}{\cos\alpha_i L - \cosh\alpha_i L}$.

From Figure 1, it can be remarked that the frequency shift curves for each bending vibration mode are similar, i.e. the differences between them are scaled by factor. By normalizing the frequency shift curves to their highest value, occurring at the clamped ends, this family of curves is reduced to a single curve, which indicates the effect of damage location. On the other hand, damage severity influences the highest value of the frequency shift alone. Consequently, the process of localization can be separated from that of severity evaluation; the damage assessment is thus possible in two steps.

2.2 Contriving the analytic relation of the frequency shift curves

Since the frequency shifts is in direct relation with the mode shape curvatures or bending moments, and the strain energy is the squared of the curvature, it is interesting to compare the frequency shift curves with that obtained from the energy distribution. Figure 3 presents this comparison for vibration modes 2 and 5; the similitude between the curves is obvious. In our researches we observed this concordance for beams with other geometrical and mechanical parameters and, which is more significant, with other support types.

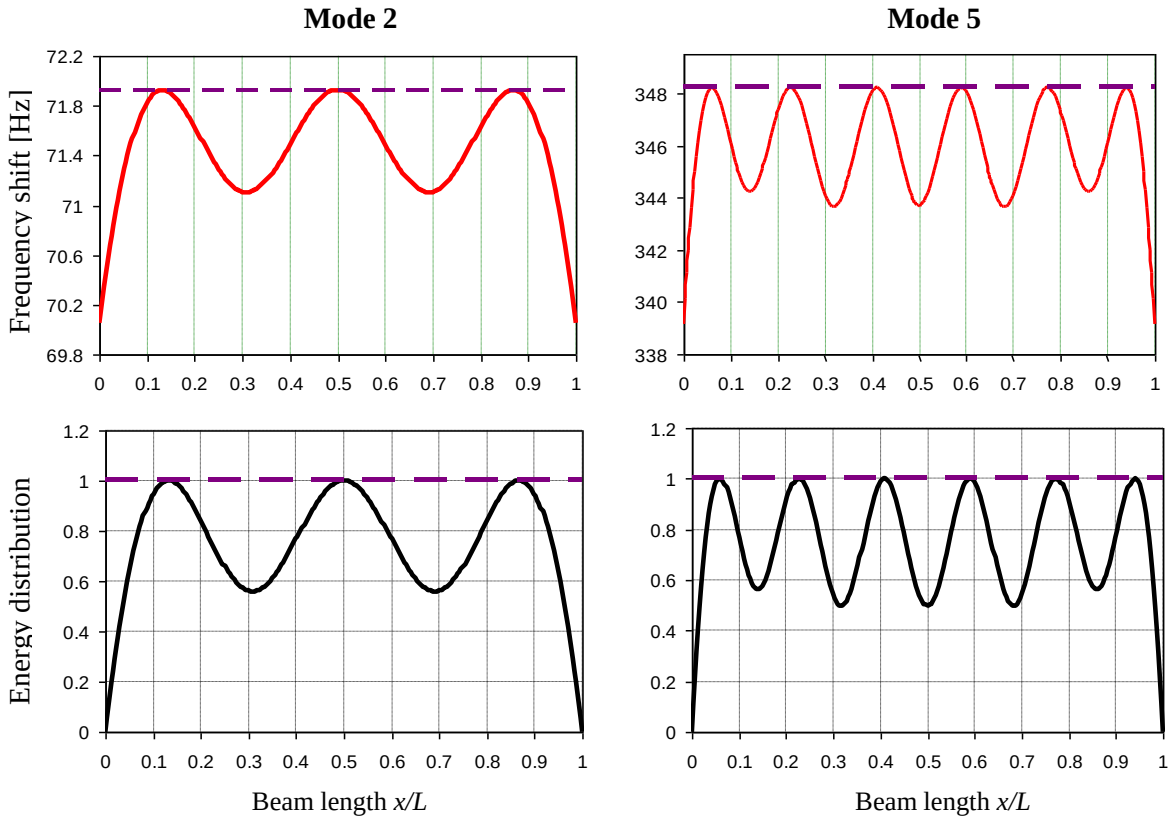

Figure 3: The frequency shift curves and energy distribution for: (a) vibration mode 2 and (b) mode 5.

The presented facts lead to the conclusion that the mathematical relation expressing the frequency shift has to involve one term depending on the damage severity and one term containing the squared of the mode shape curvature. Following numerous attempts, we reached the relation given in Eqs. (5) and (6). By defining the frequency of the weak-axis bending vibration mode i for the damaged state, depending on the maximum deflections under a unit load in the damaged and healthy state, δ_D and δ_U respectively, and the corresponding normalized mode shape curvature of the undamaged beam, is the following equations are obtained:

- at the clamped ends

$$f_{i\_D}(x) = f_{i\_U}\sqrt{\frac{\delta_U}{\delta_D}} \tag{5}$$

- at any other location.

$$f_{i\_D}(x) = f_{i\_U}\left(1 - \frac{\sqrt{\delta_D} - \sqrt{\delta_U}}{\sqrt{\delta_D}} \cdot \left(\overline{\phi_i''}(x)\right)^2\right) \tag{6}$$

The ratio between the deflections under a unit load in the damaged and healthy state just reflects the apparent increase of energy, in fact the loss of energy, so Castigliano's first theorem.

Eq. (5) is in fact a particular case of Eq. (6), where the squared of the mode shape curvature is unity. It has to be mentioned that Eq. (6) is applicable for all vibration modes and support types as it is, without further alterations. The right hand side of Eq. (6) contains information extracted from the undamaged beam, excepting the deflections δ_D and δ_U. This means that knowing the maximum deflection in the damage state, i.e. deflections δ_D and δ_U at the center of the beam, it is possible to know the frequency changes for all modes at any location x. In contrary, knowing the frequencies of different modes for the damaged and undamaged beam respectively, it is possible to determine the location and depth of the damage.

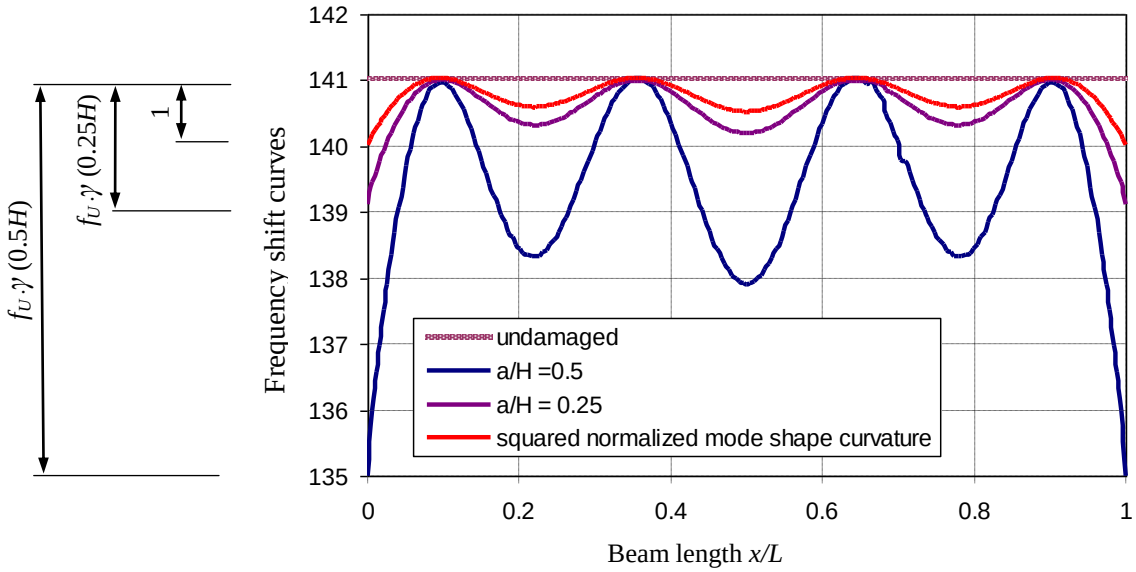

Figure 4: Frequency shift curves and squared of the mode shape curvature for bending vibration mode 3.

Figure 4 presents the frequency shift curves for two different damage depths, together with the squared normalized mode shape curvature for bending vibration mode 3. It reveals the influence of the two terms upon the natural frequency changes; herein we denoted

$$\gamma(a) = \frac{\sqrt{\delta_D(a)} - \sqrt{\delta_U}}{\sqrt{\delta_D(a)}} \tag{7}$$

where the damage severity is given by a damage of depth a. One can observe again the good fit between these curves, proving that they belong to the same family.

Eq. (6) allows us to plot surfaces representing the frequency shifts in respect to damage depth and location for any beams support type [12]. The results are similar to that obtained by the means of numerical methods such us finite element analysis [13,15]. The surfaces are obtained by numerical methods considering a multitude of points individually derived; i.e. mathematical relations that describe the curves or surfaces representing the frequency shifts are available in literature [13]. However, these relations are obtained as regression curves, which have to be derived for any beam separately. The advantage of the proposed relations is based on the fact that they consider the physical phenomenon, are simple to apply and provide accurate results.

2.3 The Damage Location Coefficients

Since the effect of a damage in any beam slice on the natural frequencies can be easily derived, it is possible to characterize each location in terms of multi-modal frequency shifts. From Eq. (6) and (7) this shift can be derived as:

$$\Delta f_i(x,a) = f_{i-U} - f_{i-D}(x,a) = f_{i-U} \cdot \gamma(a) \cdot \left(\overline{\phi_i''}(x)\right)^2 \tag{8}$$

Normalizing the frequency shift Δf_i by the frequency of the healthy beam $f_{i\text{-}U}$, one may obtain the relative frequency shift for any bending vibration mode i, as:

$$\Delta \bar{f}_i(x,a) = \gamma(a) \cdot \left(\overline{\phi_i''}(x)\right)^2 \tag{9}$$

Obviously, the relative frequency shift takes values lower than the unit. Figure 5 presents the relative frequency shifts for the first eight weak-axis bending vibration modes, highlighting the particular cases of x/L = 0.3, x/L = 0.5 and x/L = 0.7.

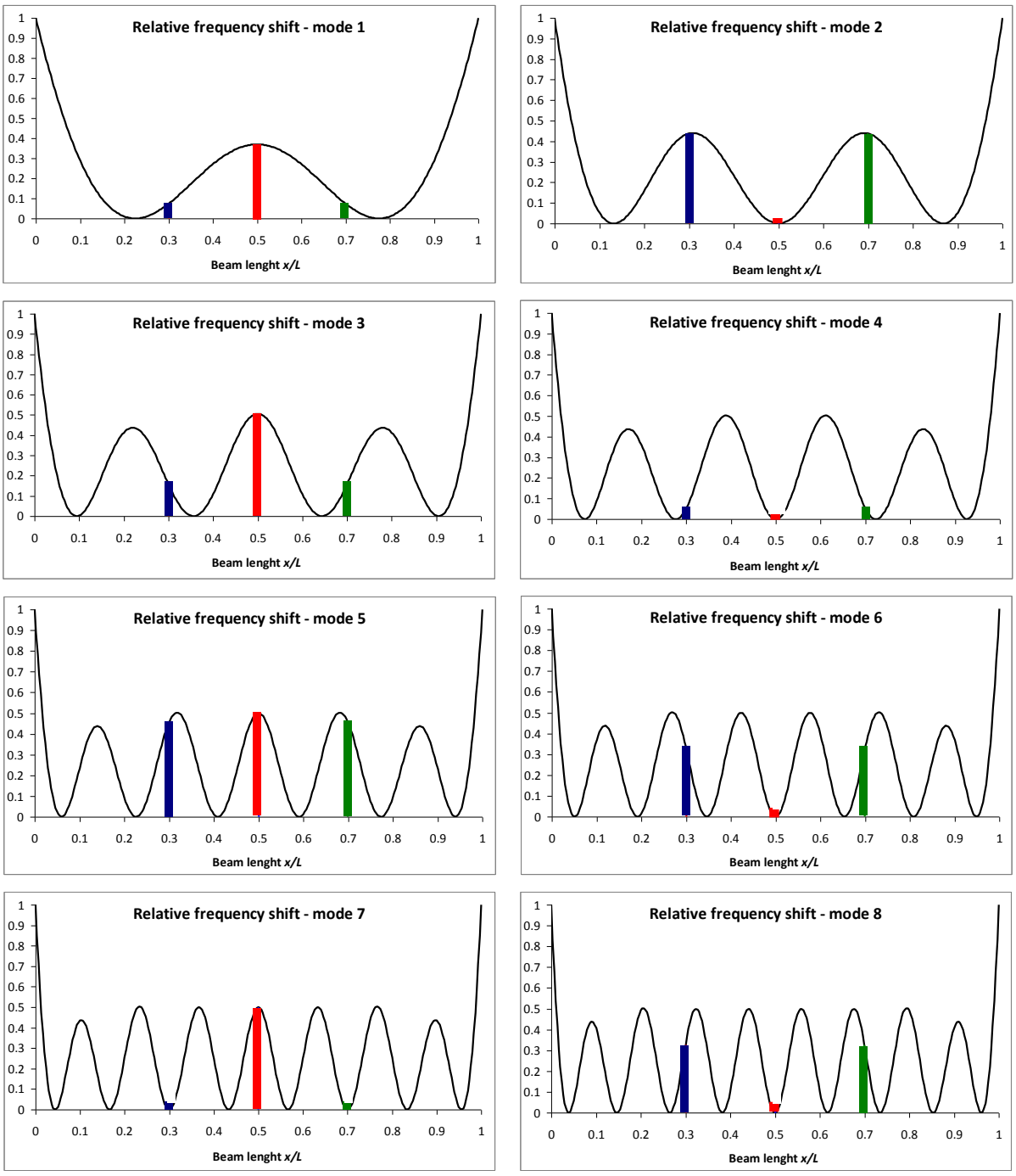

Figure 5: The relative frequency shift curves with stress on the locations x/L = 0.3, x/L = 0.5, and x/L = 0.7

Eq. (9) was used to plot the curves in Figure 5, from which one can extract the series representing the normalized frequency shift for any specific location. In Figure 6(a) the normalized frequency shifts at location x/L = 0.3 for eight vibration modes are presented. In the general case, the series has the following mathematical expression:

$$\Delta\bar{f}_1(x,a)=\gamma(a)\cdot(\bar{\phi}_1''(x))^2,\Delta\bar{f}_2(x,a)=\gamma(a)\cdot(\bar{\phi}_2''(x))^2,...,\Delta\bar{f}_8(x,a)=\gamma(a)\cdot(\bar{\phi}_8''(x))^2 \quad (10)$$

As presented in the previous section, the influence of the damage depth can be isolated by eliminating $\gamma(a)$ from Eq. (10). Moreover, if we normalize these values for each location x by dividing the values by the highest value of the series one obtain coefficients that are independent of the damage severity and take values between 0 and 1.

We denote these series as Damage Location Indicators (DLI) and the individual terms as Damage Location Coefficients (DLC). For a given location x the DLCs can be expressed as:

$$\Phi_1(x) = \frac{(\bar{\phi}_1''(x))^2}{\max((\bar{\phi}_i''(x))^2)}, \Phi_2(x) = \frac{(\bar{\phi}_2''(x))^2}{\max((\bar{\phi}_i''(x))^2)}, \ldots, \Phi_8(x) = \frac{(\bar{\phi}_8''(x))^2}{\max((\bar{\phi}_i''(x))^2)} \quad (11)$$

As it can be observed from Eq. (11), the DLCs are obtained using just information about the beam in healthy state. The DLCs uniquely characterize locations on asymmetric structures, while for symmetric structures two mirrored locations have the same value of DLC. The DLCs characterizing both locations x/L = 0.3 and x/L = 0.7 are presented in figure 6(b).

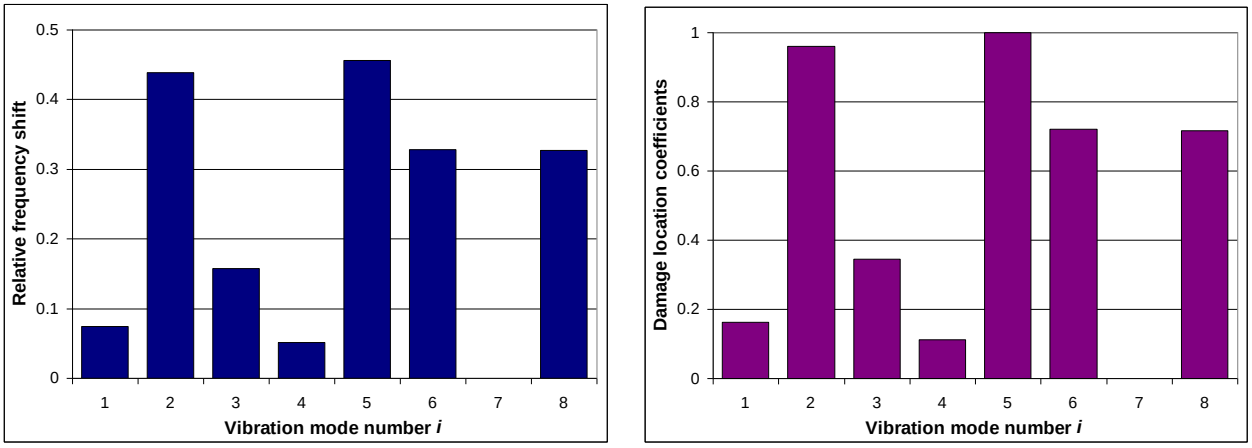

a) b)

Figure 6: The relative frequency shifts (a) and DLCs (b) for the beam with a damage located at x/L = 0.3.

If f_{i-U}^m and f_{i-D}^m are the first eight natural frequencies of the weak-axis bending vibration modes measured on a healthy beam and a beam with one damage with unknown location, respectively we can derive the relative frequency shift for the eight vibration modes, as:

$$\Delta f_1^m = f_{1-U}^m - f_{2-D}^m, \Delta f_2^m = f_{2-U}^m - f_{2-D}^m, \ldots, \Delta f_8^m = f_{8-U}^m - f_{8-D}^m \quad (12)$$

These values can be normalized by dividing them by the highest value of the series. The obtained dimensionless values are again severity-independent. We denote these series as Damage Signature and the individual terms as Measured Normalized Frequency Shifts, that are:

$$\Psi_1 = \frac{\Delta f_1^m}{\max(\Delta f_i^m)}, \Psi_2 = \frac{\Delta f_2^m}{\max(\Delta f_i^m)}, \ldots, \Psi_8 = \frac{\Delta f_8^m}{\max(\Delta f_i^m)} \quad (13)$$

These parameters have a similar meaning as the DLCs; i.e. they take also values between 0 and 1. Comparing the Damage Location Indicators $\Phi_j = \{\Phi_{1j}, \Phi_{2j}, \ldots, \Phi_{8j}\}$ for all possible locations along the beam $j = 1 \ldots m$ with the Damage Signature $\Psi = \{\Psi_1, \Psi_2, \ldots, \Psi_8\}$, obtained by measurements on the real structure, one can find the pair of vectors that best fit. The subscript j, for which the two vectors Φ and Ψ best fit, indicates the damage location.

To find the most similar vectors, we use a simple algorithm, that evaluates the ratio between pairs of terms i in the series. The idea is that for similar values the ratio is 1 and consequently its logarithm is 0. To avoid obtaining negative values, the logarithm gets an even exponent $2r$. For positive values of r, the closer the compared terms, the smaller the result. Sometimes it is convenient to use a negative exponent, that produces a dramatically increases to the lowest value; consequently the value defining the damage location is highlighted.

The similarity index, which is actually the proposed Damage Index, is:

$$DI_{LOG} = \sum_{i=1}^{n} w_i \cdot \frac{1}{\Phi_{ij}} \left(\log \frac{\Phi_{ij}}{\Psi_i} \right)^{-2r} \tag{14}$$

which indicates the presence of damage at the location at its highest value. The term w_i is a weight factor that takes values between 0 and 1 with the implicit value of unity. In case of difficulties to acquire the natural frequency of a vibration mode, or the results are improbable, the term can be diminished or even reduced to 0.

If accidentally the measured values perfectly fit those obtained by measurements, DI cannot be calculated. To avoid this, it is important to use different number of digits at the right hand side of the decimal point for the two series Φ and Ψ. Figure 7 present the variation of DI for the process of localization of a damage placed at distance x/L = 0.3 from one beam end. Figure 7(a) presents the DI values for the case of strongly altered measurement results, while Figure 7(b) presents the DI values in case of relatively well acquired frequencies.

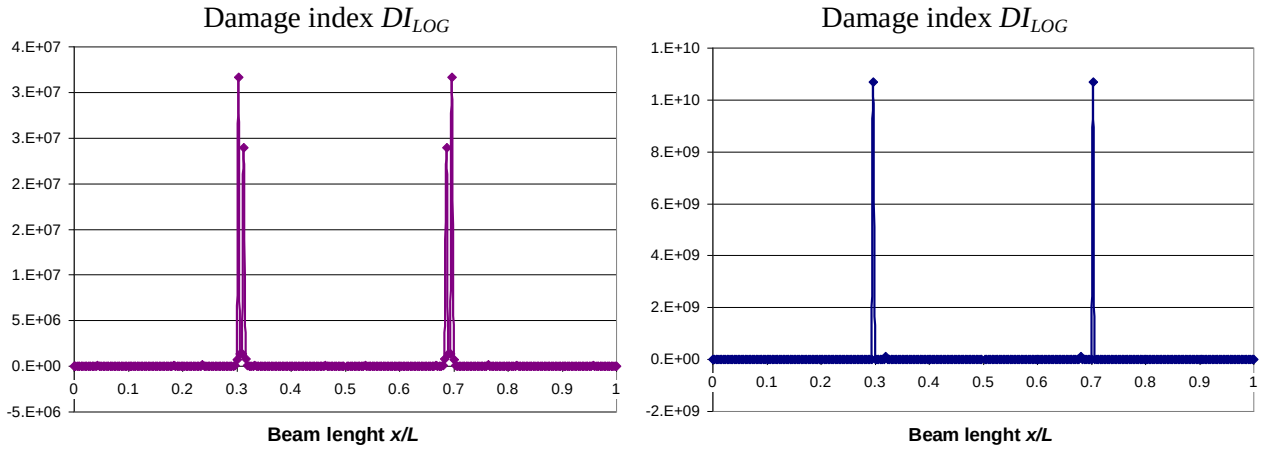

a) b)

Figure 7: Damage Index values for altered measurement data (a) and relatively accurate acquired frequencies (b) - damage placed at x/L = 0.3 from one beam end.

One observes that even using raw data the Damage Index is able to indicate precisely the damaged beam region. This makes the proposed Damage Index suitable for industrial applications in which beam-like structures or sub-structures are monitored.

3 Experimental research

3.1 Implementation of the damage localization procedure

The damage detection and localization procedure is designed to be implemented in monitoring schemes for beams in intact state or with known damages. Actually, the first measurement checks the structural integrity for the incipient stage. Afterwards, the periodic measurements evaluate the actual state and can predict damage occurrence or extension.

This paper present an algorithm where he first eight natural frequencies of the weak-axes bending vibration modes are considered. This number varies from one application to another and has to be bigger for symmetric structures. However, the minimum recommended number of monitored modes is six.

Steps to be followed in the monitoring process:

1. Initial evaluation of the structure

The first eight natural frequencies of the weak-axes bending vibration modes for the undamaged beam have to be measured. The following series is obtained:

$$A:\{ f_{1-U} ;\ f_{2-U} ; f_{3-U} ; f_{4-U} ; f_{5-U} ; f_{6-U} ; f_{7-U} ; f_{8\_U} \}$$

In case of structures in use, the actual status of the beam can be considered as start point, neglecting the possible existing cracks. Thus, only the evolution of new or developing cracks can be assessed.

2. Periodical or continuous monitoring

For the same vibration modes the frequencies have to be measured periodically. For each choose moment a series is obtained:

$$S:\{ f_{1-D} ;\ f_{2-D} ; f_{3-D} ; f_{4-D} ; f_{5-D} ; f_{6-D} ; f_{7-D} ; f_{8-D} \}$$

Changes may occur and indicates structural changes.

3. Novelty detection

Comparison with the initial estate has to be performed. The following series is obtained:

$$D:\{ \Delta f_1 ;\ \Delta f_2 ; \Delta f_3 ; \Delta f_4 ; \Delta f_5 ; \Delta f_6 ; \Delta f_7 ; \Delta f_8 \}$$

Differences representing frequency shift Δf_i indicate the presence of damage. If possible, the environmental and operational loads have to be considered.

4. Processing of data

The relative frequency shift is determined by dividing the values of D series by the ones of A series. This results in the series R

$$R:\{ \Delta f_1^{\,m} ;\ \Delta f_2^{\,m} ; \Delta f_3^{\,m} ; \Delta f_4^{\,m} ; \Delta f_5^{\,m} ; \Delta f_6^{\,m} ; \Delta f_7^{\,m} ; \Delta f_8^{\,m} \}$$

5. Computation of the Damage Signature

The values of the R series have to be normalized, by dividing all values of the series by the highest one. This results in the Damage Signature:

$$\Psi:\{ \Psi_1; \Psi_2; \Psi_3; \Psi_4; \Psi_5; \Psi_6; \Psi_7; \Psi_8 \}$$

The series' elements take positive subunit values, usually only one element takes the unit value.

6. Determining the energy distribution

Series representing squared normalized mode shape curvatures for various locations on the beam are determined by:

$$C_j:\{ \left(\overline{\phi_1''}(x)\right)^2 ; \left(\overline{\phi_2''}(x)\right)^2 ; \left(\overline{\phi_3''}(x)\right)^2 ; \left(\overline{\phi_4''}(x)\right)^2 ; \left(\overline{\phi_5''}(x)\right)^2 ; \left(\overline{\phi_6''}(x)\right)^2 ;\ \left(\overline{\phi_7''}(x)\right)^2 ; \left(\overline{\phi_8''}(x)\right)^2 \}$$

Usually the location of interest are equidistant located and have to be at least $j = 100$ to ensure a precise damage localization.

7. Computation of the Damage Location Indicators

$$\Phi_{1j}:\{ \Phi_{1\,j}; \Phi_{2\,j}; \Phi_{3\,j}; \Phi_{4\,j}; \Phi_{5\,j}; \Phi_{6\,j}; \Phi_{7\,j}; \Phi_{8\,j} \}$$

for the j locations in accordance to Eq. 11..

8. Similarity/damage identification

The Damage Signature is compared with the derived Damage Location Indicators by using Eq. (14). The damage is presumed to be at the location for which the DI_{LOG} take its highest value. However, the indicator diagram should be carefully examined to assure that no ambiguous results are obtained. Normally the value of r in the DI_{LOG} is equal to unity, but for disambiguation the value can be increased.

Following this procedure the damage is localized with high accuracy. While the procedure imposes no human interaction, it can be easily implemented in a program for automated damage recognition [16]. For the case of multiple damages, the method of superposition can be applied [17], so that the system can recognize even multiple cracks if the database containing DLIs is extended with other scenarios.

Knowing the frequency shifts and damage location, its severity $\gamma(a)$ can be now extracted as single unknown from Eq. (9). Thereafter, damage depth a can be derived using algorithms described in literature, see references [7] and [18].

3.2 Numerical results

A series of experimental tests were performed on steel beams to validate the suitability of the procedure that makes use of the proposed Damage Index. This paper presents results obtained on beams fixed at both ends. The equipment used for the vibration signal acquisition, presented in figure 8, consists of a laptop, a NI cDAQ-9181 single slot chassis with Ethernet connection, a NI 9234 four-channel dynamic signal acquisition module and two Kistler 8772A10M10 piezoelectric accelerometers. The accelerometers were placed on the beam in positions permitting a reliable signal acquisition for the first eight weak-axis bending vibration modes. A virtual instrument was designed in the LabVIEW environment, capable to acquire the time history of acceleration and extract the natural frequencies with high accuracy, as early damage detection implies observation of small frequency changes.

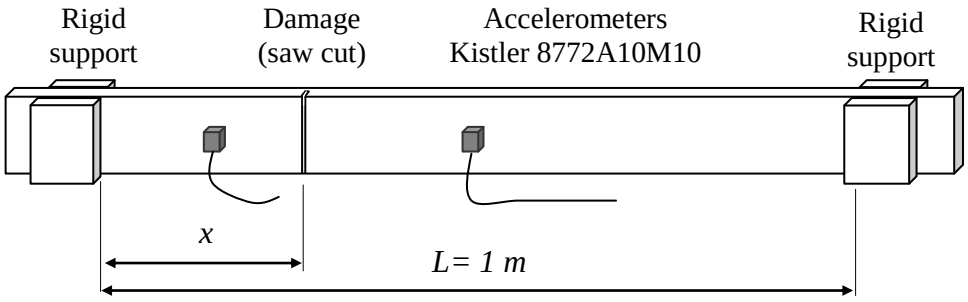

Figure 8: Damage index values for altered measurement data (a) and relatively accurate acquired frequencies (b) - damage placed at x/L = 0.3 from one beam end.

The real beams have identical physical, mechanical and geometrical characteristics like that presented in section 2, used in finite element analysis. A thin saw cut, with a width less than 1 mm and depth around 2 mm, was made to simulate the damage at a location situated at one third from the left beam's fixed end. The saw cut acceptably simulates a breathing crack, while significant loss of mass is avoided and differences between open and closed cracks is less important. A detailed study about this topic is presented in reference [19]. The excitation is produced by hitting the beam with a hammer.

Measurement results obtained for the first eight vibration modes, for intact beam, are presented in Table 1, in which frequencies obtained analytically and by means of the finite element analysis are also listed. One can observe the good matching of these results.

For the damaged case, as expected, the measurement indicated a frequency diminishing. The results of the damaged beam, as well as the results obtained by measurements on the healthy beam healthy and are presented in table 2,. By performing the first five steps of the procedure described above, we obtained the Damage Signature. The similarity test with the DLIs for three hundred equidistant locations indicated that the highest value of the DI_{LOG} is obtained for j = 87, i.e. the saw cut is placed at distance x/L = 0.29 from one of the beam's fixed ends. The comparative values of the Damage Signature Ψ and the DLCs Φ_{87} are also presented in table 2. Dimensional measurements confirmed the location of damage, which proves the method's reliability.

Mode number i	Frequency [Hz] analytic calculus	finite element analysis	experimental
1	25.942358	26.099351	25.612542
2	71.511108	71.926667	71.131492
3	140.190365	140.991467	140.325688
4	231.741795	233.070571	230.491022
5	346.182261	348.205537	344.525590
6	483.510757	486.420653	485.038719
7	643.727340	647.735055	640.716628
8	826.832006	832.155573	830.300510

Table 1: First eight natural frequencies of the healthy beam

Mode number i	Measured frequency [Hz] undamaged $f_{i\text{-}U}$	damaged $f_{i\text{-}D}$	Damage signature Ψ_i	Damage location coefficient Φ_{i87}
1	25.612542	25.597815	0.1340	0.13358
2	71.131492	70.825555	1	1
3	140.325688	140.035074	0.4837	0.48151
4	230.491022	230.452069	0.0382	0.03919
5	344.525590	343.165747	0.9173	0.91771
6	485.038719	483.015623	0.9697	0.96960
7	640.716628	640.541072	0.0637	0.06377
8	830.300510	828.678933	0.4562	0.45403

Table 2: Results of the damage localization process

Graphical representations for all values obtained in the similarity analysis (i.e. for all location $j = 1\ldots300$ considered along the beam) are presented in Figure 9. Figure 9(a) depicts the values obtained by means of the proposed Damage Index and Figure 9(b) shows the values obtained by using the Kullback-Leibler Divergence; obviously this Damage Index more clearly indicates the damage location in comparison with other similarity estimators [19]. On the other hand, the DLCs are reliable patters characterizing the damage location; this is evidenced in our prior researches for a cantilever, see for instance reference [20].

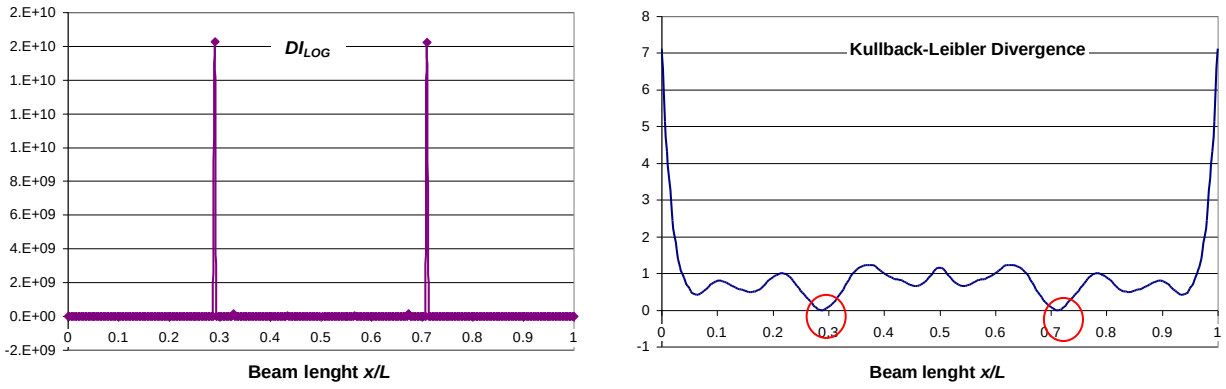

a) b)

Figure 9: Damage localization process utilizing: (a) the proposed Damage Index, and (b) the Kullback-Leibler Divergence.

The procedure was tested on beams with different support types, of various damages locations and depths, all identifications being successfully performed.

4 Conclusion

The frequency changes due to a transversal discontinuity in beams depend on the modal strain energy stored in the affected slice. Because the beam's stiffness decrease due to a given damage is the same for any bending vibration mode, the maximum effect upon the frequency shifts is similar in all modes, but scaled by the value of the squared wave number λ_i. These changes occur at the location where the stored energy level takes its highest value (in the fixed ends for the double clamped beam in the analyzed case), while in all other locations the frequency changes depend on the modal strain energy distribution. Therefore, there is no sensitive or insensitive bending vibration mode, but we can affirm that there are sensitive locations, in respect to the vibration mode and boundary conditions. This paper proposes a mathematical relation that makes the link between the frequency of the healthy beam, the energy distribution (i.e. the squared mode shape curvature) and the damage severity.

Damage localization and severity evaluation are separable, while the stiffness reduction controls the severity and the squared mode shape curvatures control the local sensitivity.

For the same damage scenario, a single location along the beam present different "sensitivities" in different vibration modes, imposed by the beam curvature in each mode. This makes the local values of the squared mode shape curvatures in several modes, i.e. the proposed Damage Location Coefficients, patterns able to characterize any location. This constitutes the basis of the proposed damage localization procedure.

A new damage index, DI_{LOG} is proposed. It compares the Damage Signatures obtained from measurements with numerous patterns analytically defined from information from the healthy beam alone. The position for which the highest value is obtained indicates the damage location. This damage index is able to localize multiple cracks if patterns for these scenarios are developed based on the superposition principle.

Acknowledgements

The work has been funded by the Sectoral Operational Programme Human Resources Development 2007-2013 of the Ministry of European Funds through the Financial Agreement POSDRU/159/1.5/S/132395.

References

[1] S.W. Doebling, C.R. Farrar, M.B. Prime, D.W. Shevitz, *Damage identification and health monitoring of structural and mechanical systems from changes in their vibration characteristics: A literature review*. Los Alamos National Laboratory Report, LA-13070-MS. Los Alamos (1996).

[2] H. Sohn, C.R. Farrar, F.M. Hemez, D.D. Shunk, D.W. Stinemates, B.R.Nadler, *A review of structural health monitoring literature: 1996–2001*. Los Alamos National Laboratory report, LA-13976-MS. Los Alamos (2003).

[3] M.I. Friswell, *Damage identification using inverse methods*, Philosophical Transactions of the Royal Society A, Vol. 365, No. 1851, Royal Society Publishing (2007), pp. 393–410.

[4] C.P. Fritzen, *Vibration-Based Techniques for Structural Health Monitoring*, in: D. Balageas, C.P. Fritzen, A. Güemes (Eds.), Structural Health Monitoring, ISTE, London (2006), pp. 45-224.

[5] M.I. Friswell, J.E.T. Penny, *Crack Modeling for Structural Health Monitoring*, Structural Health Monitoring, Vol. 1, No. 2, SAGE Publications (2002), pp. 138-146.

[6] A.D. Dimarogonas, *Vibration of cracked structures: a state of the art review*, Eng. Fract. Mech. 55 (1996), pp. 831–857.

[7] W. Ostachowicz, M. Krawczuk, *On modeling of structural stiffness loss due to damage*. *Proceedings of 4th International Conference, DAMAS 2001, Cardiff, Wales, UK, 2001 June 25-28*, Cardiff (2001), pp. 185–199.

[8] S. Christides, ASD. Barr, *One-Dimensional Theory of Cracked Bernoulli-Euler Beams*, International Journal of Mechanical Sciences, Vol. 26, Elsevier (1984), pp. 639-648.

[9] G. Yan, A. De Stefano, E. Matta, R. Feng, *A novel approach to detecting breathing-fatigue cracks based on dynamic characteristics*, Journal of Sound and Vibration, Vol. 332, No. 1, Elsevier (2013), pp. 407–422.

[10] T.G. Chondros, A.D. Dimarogonas, J. Yao, *A continuous cracked beam vibration theory*, Journal of Sound and Vibration, Vol. 215, No. 10, Elsevier (1998), pp. 17–34.

[11] M. Afshari, D.J. Inman, *Continuous crack modeling in piezoelectrically driven vibrations of an Euler–Bernoulli beam*, Journal of Vibration and Control, Vol. 19, No. 3, SAGE Publications (2013), pp. 341–355.

[12] G.R. Gillich, Z.I. Praisach, *Modal identification and damage detection in beam-like structures using the power spectrum and time–frequency analysis*, Signal Processing, Volume 96, Part A, March 2014, Pages 29–44

[13] E. Ekinovic, *An approximate technique for damage identification in beams using shifts in natural frequencies*, *Proceedings of The 22nd International Conference on Noise and Vibration Engineering, Leuven, Belgium, 2010 September 20-22,* Leuven (2010), paper 0024.

[14] M. Caoa, P. Qiao, *Novel Laplacian scheme and multiresolution modal curvatures for structural damage identification,* Mechanical Systems and Signal Processing 23 (2009), pp. 1223–1242

[15] A.V. Deokar, V.D. Wakchaure, *Experimental Investigation of Crack Detection in Cantilever Beam Using Natural Frequency as Basic Criterion*, *Proceedings of The 2nd International Conference on Current Trends in Technology - NUiCONE 2011, Ahmedabad, India, 2011 December 08-10*, Ahmedabad (2011), pp. 1-6.

[16] PF Minda, ZI Praisach, AA Minda, GR Gillich, *Methods of interpreting the Results of Vibration Measurements to locate Damages in Beams***,** Applied Mechanics and Materials, Vol. 430, Trans Tech Publications (2013), pp. 84-89

[17] Z.I. Praisach, G.R. Gillich, *Influence of multiple cracks upon the dynamic behaviour of beams*, in A. Zingoni, editor, *Proceedings of The Fifth International Conference on Structural Engineering, Mechanics and Computation, Cape Town, South Africa, 2013 September 2-4*, Cape Town (2013), pp. 2199-2204.

[18] Z.I. Praisach, G.R. Gillich, C. Protocsil, F. Muntean, *Evaluation of Crack Depth in Beams for known Damage Location based on Vibration Modes Analysis*, Applied Mechanics and Materials, Vol. 430, Trans Tech Publications (2013), pp. 90-94.

[19] P.F. Minda, Z.I. Praisach, N. Gillich, A.A. Minda, G.R. Gillich, *On the Efficiency of Different Dissimilarity Estimators Used in Damage Detection*, Romanian Journal of Acoustics and Vibration, Vol. 10, No. 1, SRA Press (2013), pp. 15-18.

[20] G.R. Gillich, Z.I. Praisach, *Damage-patterns-based method to locate discontinuities in beams*, in T. Kundu, editor, *Proceedings of SPIE 8695, Health Monitoring of Structural and Biological Systems, San Diego, California, USA, 2013 March 11-14*, San Diego (2013), paper 869532.